Techniques For Sway Control Of A Double-Pendulum-Type Overhead Crane

M.A. Ahmad, R.M.T. Raja Ismail, M.S. Ramli, A.N.K. Nasir, N.M. Abd Ghani And N.H. Noordin

Control and Instrumentation Research Group (COINS)
Faculty of Electrical and Electronics Engineering
Universiti Malaysia Pahang,
Pekan, 26600, Pahang, Malaysia

Abstract - **This paper presents investigations into the development of input shaping techniques for swaying control of a double-pendulum-type overhead crane (DPTOC) system. A nonlinear DPTOC system is considered and the dynamic model of the system is derived using the Euler-Lagrange formulation. An unshaped bang-bang input force is used to determine the characteristic parameters of the system for design and evaluation of the input shaping control techniques. The positive and modified specified negative amplitude (SNA) input shapers with the derivative effects respectively are designed based on the properties of the system. Simulation results of the response of the DPTOC system to the shaped inputs are presented in time and frequency domains. Performances of the control schemes are examined in terms of sway angle reduction and time response specifications. Finally, a comparative assessment of the proposed control techniques is presented and discussed.**

Keywords: *Double-pendulum-type overhead crane, anti-sway control, positive input shaping, negative input shaping.*

I. INTRODUCTION

The natural sway of crane payloads causes safety hazards, time delays and difficulty in positioning. Much of the previous work on crane control has attempted to address this issue using techniques based around a single-pendulum model of a crane. If a computer controller is utilized, then the time-optimal commands that result in zero residual vibration can be generated. When feedback is available, adaptive controllers and combination open- and closed-loop control is possible (Kim and Singhose, 2006). The performance of precision motion depends on damping capacity of the system. The damping capability of a dynamical system can be enhanced by passive or active damping methods. In the passive approach, oscillation damping is increased by deploying external dampers such as dashpots or viscous dampers (Yang et al., 2006). Feedback control can also be used as an active approach in a wide band of insensitivity.

Another approach is feed-forward control techniques. Feed-forward control schemes are mainly developed for sway suppression and involve developing the control input through consideration of the physical and swaying properties of the system, so that system sways at response modes are reduced. The earliest incarnation of this self-canceling command generation was developed by (Smith, 1957) but his technique was extremely sensitive to modeling errors (Robertson and Singhose, 2005). Singer and Seering developed reference commands that were robust enough to be effective on a wide range of systems (Singer and Seering, 1990). This new robust technique is named as input shaping.

Input shaping is implemented by convolving a sequence of impulses, an input shaper, with a desired system command to produce a shaped input that produces self-canceling command signal (Singhose et al., 1997). Input shaper is designed by generating a set of constraint equations which limit the residual vibration, maintain actuator limitations, and ensure some level of robustness to modeling errors (Singhose and Singer, 1996). The process has the effect of placing zeros near the locations of the flexible poles of the oscillatory system. In the input shaper, the amplitudes and time locations of the impulses are determined by solving the set of constraints (Gürleyük, 2007).

Most existing crane control systems are designed to maximize speed, in an attempt to minimize system sway and achieve good positional accuracy in a minimum duration (Gürleyük and Cinal, 2007). High stiffness can be achieved by using short rope or heavy carrier head. As a result, such cranes are usually heavy with respect to its payload. This limits the speed of operation of transportation, increases size of driving motor and energy consumption (Mohamed, et al., 2005). In filtering techniques, a filtered torque input is developed on the basis of extracting the input energy around the natural frequencies of the system. These include filtering techniques based on low-pass, band-stop and notch filters (Singhose et al., 1995; Tokhi and Poerwanto, 1996).

In another issue, using input shaper scheme, a response without sway can be achieved, however, with a slight time delay approximately equal to the length of the impulse sequence. With more impulses, the system becomes more robust to sway mode parameter changes, but this will result in longer delay in the system response. To reduce the delay in the system response, negative amplitude input shapers have been introduced and investigated in vibration control. By allowing the shaper to contain negative impulses, the shaper duration can be shortened, while satisfying the same robustness constraint. A significant number of negative shapers for vibration control have also been proposed. These include negative unity-magnitude (UM) shaper, specified-negative-amplitude (SNA) shaper, negative zero-vibration (ZV) shaper, negative zero-vibration-derivative (ZVD) shaper and negative zero-vibration-derivative-derivative (ZVDD) shaper (Mohamed et al., 2006).

This paper presents investigations into the development of control schemes for anti-swaying control of a double-pendulum-type overhead crane (DPTOC) system. A nonlinear DPTOC system is considered and the dynamic model of the system is derived using the Euler-Lagrange formulation. An unshaped bang-bang force input is used to determine the characteristic parameters of the system for design and evaluation of the input shaping control techniques. The positive zero-sway-derivative-derivative (PZSDD) and new modified specified negative amplitude zero-sway-derivative-derivative (SNA-ZSDD) input shapers are then designed based on the properties of the system for anti-sway control. Simulation results of the response of the DPTOC system to the shaped inputs are presented in time and frequency domains. Performances of the shapers are examined in terms of swing angles reduction and time response specifications. Moreover, a comparative assessment of the effectiveness of the positive and negative input shapers in suppressing sway of the DPTOC system is discussed.

The rest of this paper is structured in the following manner. The next section provides a brief description of the double pendulum-type overhead crane system considered in this study. Section 3 describes the modelling of the system derived using Euler-lagrange formulation whilst Section 4 describes the design of both positive and negative input shaping schemes. Implementation results and comparative assessment is reported in Section 5. Finally, concluding remarks are offered in the last section.

II. THE DOUBLE-PENDULUM-TYPE OVERHEAD CRANE SYSTEM

The DPTOC system with its hook and load considered in this work is shown in Figure 1, where x is the trolley position, m is the trolley mass, and m_1 and m_2 are the hook and load mass respectively. θ_1 is the hook swing angle, θ_2 is the load swing angle, l_1 and l_2 are the cable length of the hook and load, respectively, and F is the trolley drive force. In this simulation, the hook and load can be considered as point masses.

Figure 1: Description of the DPTOC system.

III. DYNAMIC MODELING OF THE DOUBLE-PENDULUM-TYPE OVERHEAD CRANE

This section provides a brief description on the modeling of the DPTOC system, as a basis of a simulation environment for development and assessment of the feed-forward control techniques. The Euler-Lagrange formulation is considered in characterizing the dynamic behavior of the crane system incorporate payload.

By Lagrange's equations, the dynamic model of the DPTOC system, shown in Figure 1, is assumed to have the following form (Spong, 1997)

$$M(q)\ddot{q} + C(q,\dot{q})\dot{q} + G(q) = \bar{\tau} \qquad (1)$$

where the matrices $M(q) \in \Re^{3\times3}$, $C(q,\dot{q}) \in \Re^{3\times3}$, and $G(q) \in \Re^3$ represent the inertia, Centrifugal-Coriolis terms, and gravity, respectively, and are defined as

$$M(q) = \begin{bmatrix} m+m_1+m_2 & (m_1+m_2)l_1\cos\theta_1 \\ (m_1+m_2)l_1\cos\theta_1 & (m_1+m_2)l_1^2 \\ m_2l_2\cos\theta_2 & m_2l_1l_2\cos(\theta_1-\theta_2) \end{bmatrix}$$
$$\begin{bmatrix} m_2l_2\cos\theta_2 \\ m_2l_1l_2\cos(\theta_1-\theta_2) \\ m_2l_2^2 \end{bmatrix} (2)$$

$$C(q,\dot{q}) = \begin{bmatrix} 0 & -(m_1+m_2)l_1\dot{\theta}_1\sin\theta_1 \\ 0 & 0 \\ 0 & -m_2l_1l_2\dot{\theta}_1\sin(\theta_1-\theta_2) \end{bmatrix}$$

$$\begin{bmatrix} -m_2 l_2 \dot{\theta}_2 \sin\theta_2 \\ m_2 l_1 l_2 \dot{\theta}_1 \sin(\theta_1 - \theta_2) \\ 0 \end{bmatrix} \quad (3)$$

$$G(q) = \begin{bmatrix} 0 & (m_1 + m_2)gl_1 \sin\theta_1 & m_2 gl_2 \sin\theta_2 \end{bmatrix}^T \quad (4)$$

where g is the gravity effect. The state vector q and the control vector $\bar{\tau}$, are defined as

$$q = \begin{bmatrix} x & \theta_1 & \theta_2 \end{bmatrix}^T$$
$$\bar{\tau} = \begin{bmatrix} F & 0 & 0 \end{bmatrix}^T$$

After rearranging (1) and multiplying both sides by M^{-1}, one obtains

$$\ddot{q} = M^{-1}(-C\dot{q} - G + \bar{\tau}) \quad (5)$$

where M^{-1} is guaranteed to exist due to $\det(M) > 0$.

In this study the values of the parameters are defined as m=5 kg, m_1=2 kg, m_2=5 kg, l_1=2 m, l_2=1 m and g=9.8 m-s^{-2} (Liu et al., 2006).

IV. INPUT SHAPING CONTROL SCHEMES

The design objectives of input shaping are to determine the amplitude and time locations of the impulses in order to reduce the detrimental effects of system flexibility. These parameters are obtained from the natural frequencies and damping ratios of the system. The input shaping process is illustrated in Figure 2.
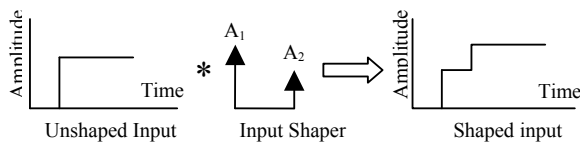
Figure 2: Illustration of input shaping technique.

Generally, a vibratory system of any order can be modelled as a superposition of second order systems each with a transfer function

$$G(s) = \frac{\omega^2}{s^2 + 2\zeta\omega s + \omega^2}$$

where ω is the natural frequency of the vibratory system and ζ is the damping ratio of the system. Thus, the response of the system in time domain can be obtained as

$$y(t) = \frac{A\omega}{\sqrt{1-\zeta^2}} \exp^{-\zeta\omega(t-t_0)} \sin\left(\omega\sqrt{1-\zeta^2}(t-t_0)\right)$$

where A and t_0 are the amplitude and the time location of the impulse respectively. The response to a sequence of impulses can be obtained by superposition of the impulse responses. Thus, for N impulses, with $\omega_d = \omega\left(\sqrt{1-\zeta^2}\right)$, the impulse response can be expressed as

$$y(t) = M \sin(\omega_d t + \beta)$$

where

$$M = \sqrt{\left(\sum_{i=1}^{N} B_i \cos\phi_i\right)^2 + \left(\sum_{i=1}^{N} B_i \sin\phi_i\right)^2},$$

$$B_i = \frac{A_i \omega}{\sqrt{1-\zeta^2}} \exp^{-\zeta\omega(t-t_0)}, \qquad \phi_i = \omega_d t_i$$

and A_i and t_i are the amplitudes and time locations of the impulses.

The residual single mode vibration amplitude of the impulse response is obtained at the time of the last impulse, t_N as

$$V = \sqrt{V_1^2 + V_2^2} \quad (6)$$

where

$$V_1 = \sum_{i=1}^{N} \frac{A_i \omega_n}{\sqrt{1-\zeta^2}} \exp^{-\zeta\omega_n(t_N - t_i)} \cos(\omega_d t_i) \; ;$$

$$V_2 = \sum_{i=1}^{N} \frac{A_i \omega_n}{\sqrt{1-\zeta^2}} \exp^{-\zeta\omega_n(t_N - t_i)} \sin(\omega_d t_i)$$

To achieve zero vibration after the last impulse, it is required that both V_1 and V_2 in Equation (6) are independently zero. This is known as the zero residual vibration constraints. In order to ensure that the shaped command input produces the same rigid body motion as the unshaped reference command, it is required that the sum of amplitudes of the impulses is unity. This yields the unity amplitude summation constraint as

$$\sum_{i=1}^{N} A_i = 1 \qquad (7)$$

In order to avoid response delay, time optimality constraint is utilised. The first impulse is selected at time $t_1 = 0$ and the last impulse must be at the minimum, i.e. min (t_N) The robustness of the input shaper to errors in natural frequencies of the system can be increased by taking the derivatives of V_1 and V_2 to zero. Setting the derivatives to zero is equivalent to producing small changes in vibration corresponding to the frequency changes. The level of robustness can further be increased by increasing the order of derivatives of V_1 and V_2 and set them to zero. Thus, the robustness constraints can be obtained as

$$\frac{d^i V_1}{d\omega_n{}^i} = 0 \; ; \; \frac{d^i V_2}{d\omega_n{}^i} = 0 \qquad (8)$$

Both the positive and SNA input shapers are designed by considering the constraints equations. The following section will further discuss the design of the positive and SNA input shapers.

A. Positive Input Shaper

The requirement of positive amplitudes for the input shapers has been used in most input shaping schemes. The requirement of positive amplitude for the impulses is to avoid the problem of large amplitude impulses. For the case of positive amplitudes, each individual impulse must be less than one to satisfy the unity magnitude constraint. In order to increase the robustness of the input shaper to errors in natural frequencies, the positive zero-sway-derivative-derivative (PZSDD) input shaper, is designed by solving the derivatives of the system vibration equation. This yields a four-impulse sequence with parameter as

$$t_1 = 0, \; t_2 = \frac{\pi}{\omega_d} , \; t_3 = \frac{2\pi}{\omega_d} , \; t_4 = \frac{3\pi}{\omega_d}$$

$$A_1 = \frac{1}{1+3K+3K^2+K^3} , \; A_2 = \frac{3K}{1+3K+3K^2+K^3}$$

$$A_3 = \frac{3K^2}{1+3K+3K^2+K^3} , \; A_4 = \frac{K^3}{1+3K+3K^2+K^3} \quad (9)$$

where

$$K = e^{-\frac{\zeta\pi}{\sqrt{1-\zeta^2}}} , \; \omega_d = \omega_n\sqrt{1-\zeta^2}$$

(ω_n and ζ representing the natural frequency and damping ratio respectively) and t_j and A_j are the time location and amplitude of impulse j respectively.

B. Modified SNA Input Shaper

In order to achieve higher robustness for positive input shaper, the duration of the shaper is increased and thus, increases the delay in the system response. By allowing the shaper to contain negative impulses, the shaper duration can be shortened, while satisfying the same robustness constraint. To include negative impulses in a shaper requires the impulse amplitudes to switch between 1 and -1 as

$$A_i = (-1)^{i+1}; \; i = 1,\dots,n \qquad (10)$$

The constraint in (10) yields useful shapers as they can be used with a wide variety of inputs. However, the increase in the speed of system response achieved using the SNA input shapers is at the expense of some tradeoffs and penalties. The shapers containing negative impulses have tendency to excite unmodeled high modes and they are slightly less robust as compared to the positive shapers. Besides, negative input shapers require more actuator effort than the positive shapers due to high changes in the set-point command at each new impulse time location.

To overcome the disadvantages, the modified SNA input shaper is introduced, whose negative amplitudes can be set to any value at the centre between each normal impulse sequences. In this technique, the previous SNA input shaper (Mohamed et al., 2006) has been modified by locating the negative amplitudes at the centre between each positive impulse sequences with even number of total impulses. This will result the shaper duration to one-fourth of the sway period of an undamped system as shown in Figure 3. The modified SNA-ZSDD shaper is applied in this work by adding more negative impulses in order to enhance the robustness capability of the controller while increasing the speed of the system response. Moreover, by considering the form of modified SNA-ZSDD shaper shown in Figure 3, the amplitude summation constraints equation can be obtained as

$$2a + 2c - 2b - 2d = 1 (11)$$

The values of *a, b, c* and *d* can be set to any value that satisfy the constraint in (11). However, the suggested values of *a, b, c* and *d* are less than 1 to avoid the increase of the actuator effort.
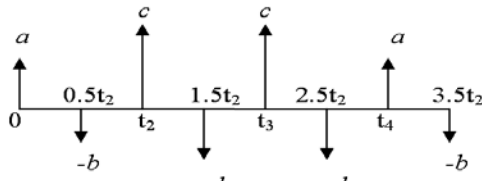
Figure 3: Modified SNA-ZSDD shaper.

V. IMPLEMENTATION AND RESULTS

In this investigation, input shaping control schemes are implemented and tested within the simulation environment of the DPTOC system and the corresponding results are presented. The bang-bang input force of ±1 N is applied to the trolley of the DPTOC. For the sway suppression schemes, positive ZSDD and modified SNA-ZSDD are designed based on the sway frequencies and damping ratios of the DPTOC system. The first three modes of sway of the system are considered, as these dominate the dynamic of the system. The responses of the DPTOC system to the unshaped input were analysed in time-domain and frequency domain (spectral density). These results were considered as the system response to the unshaped input and will be used to evaluate the performance of the input shaping techniques.

Simulation results for the unshaped input have shown that a chattering about ±0.05 m occurred at the steady-state for the trolley position. Moreover, a significant sways occur at the hoisting angles of the hook cable and load cable during the movement of the trolley. The hoisting angle responses were found to oscillate between ±0.03 rad for hook cable and ±0.04 rad for load cable. The sway frequencies for both hook cable and load cable were obtained as 0.4883 Hz, 1.099 Hz and 1.587 Hz for the first three modes of sway.

In the case of input shaping control schemes, positive and modified SNA-ZSDD shapers were designed for three modes utilising the properties of the system. With the natural frequencies of 0.4883 Hz, 1.099 Hz and 1.587 Hz, the time locations and amplitudes of the impulses for positive ZSDD shaper were obtained by solving (9). However, the amplitudes of the modified SNA-ZSDD shaper were deduced as [0.3 –0.1 0.5 –0.2 0.5 –0.2 0.3 –0.1] while the time locations of the impulses were located at the half of the time locations of positive ZSDD shaper as shown in Figure 3.

Figures 4-8 show the trolley position, swing angle of hook and load cable response and its power spectral density. Table 1 summarises the levels of sway reduction of the system responses at the first three modes. Higher levels of sway reduction were obtained using positive ZSDD shaper as compared to the case with modified SNA-ZSDD shaper. However, with modified SNA-ZSDD shaper, the system response is faster. The corresponding rise time, settling time and overshoot of the trolley

position response for positive and modified SNA-ZSDD shapers is depicted in Table 1.

By comparing the results presented in Table 1, it is noted that the higher performance in the reduction of sway of the system is achieved using positive ZSDD shaper. This is observed and compared to the modified SNA-ZSDD shaper at the first three modes of sway. For comparative assessment, the levels of sway reduction of the hoisting angles of the hook and load cables using both positive and modified SNA-ZSDD shapers are shown with the bar graphs in Figure 9 and Figure 10, respectively. The result shows that, highest level of sway reduction is achieved in control schemes using the positive ZSDD shaper, followed by the modified SNA-ZSDD shaper for all modes of sway, for both of hook and load swing angles. Therefore, it can be concluded that the positive ZSDD shapers provide better performance in sway reduction as compared to the modified SNA-ZSDD shapers in overall.

Comparisons of the specifications of the trolley position response of input shaping control schemes using both positive and modified SNA-ZSDD shapers are summarised in Figure 11 for the rise times and settling times. It is noted that settling time of the cart position response by using the modified SNA-ZSDD shaper is faster than the case using the positive ZSDD shaper. It shows that, in term of settling time, the speed of the system response can be improved by using a negative impulse input shapers.
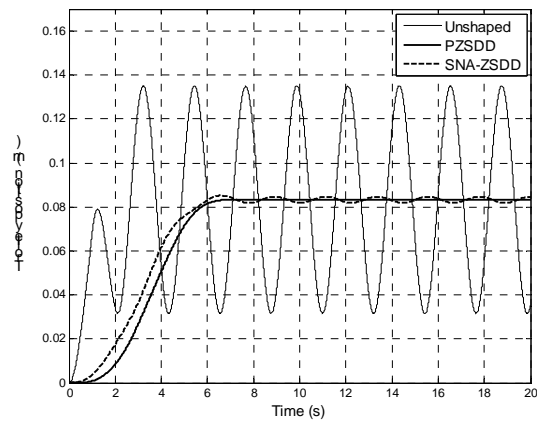

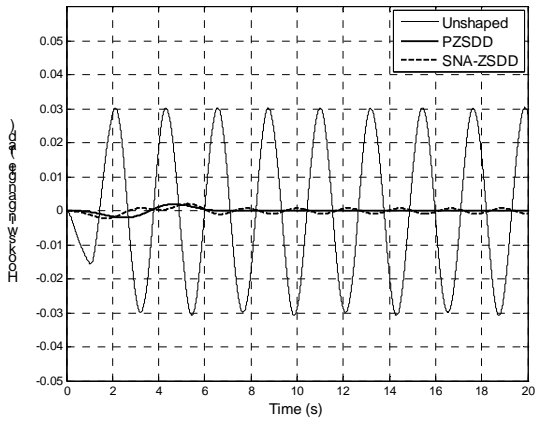Figure 4: Response of the trolley position.
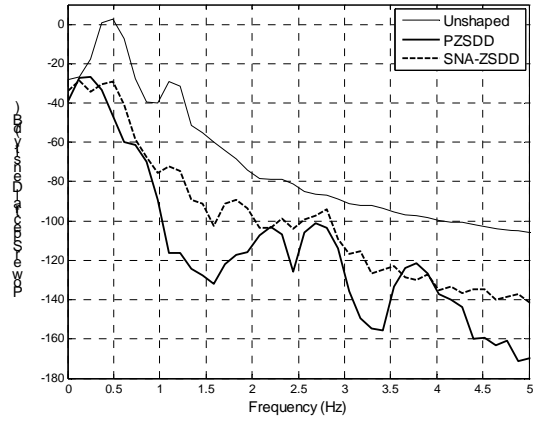
Figure 5: Response of the hook swing angle.

Figure 6: Response of the load swing angle.

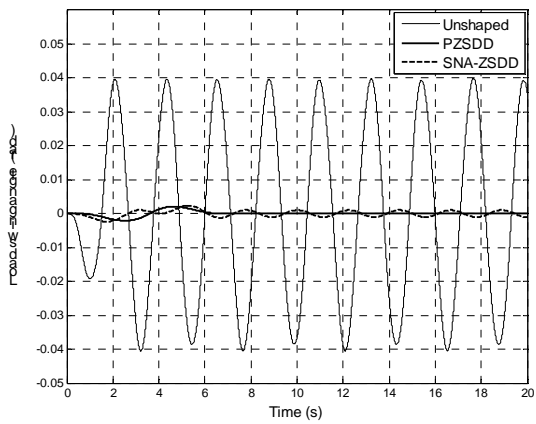Figure 7: Spectral density of the hook swing angle.

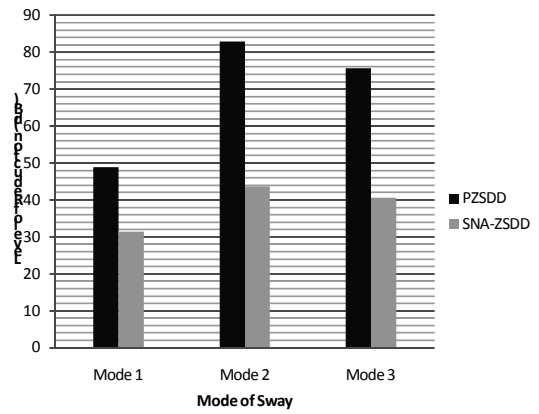Figure 8: Spectral density of the load swing angle.
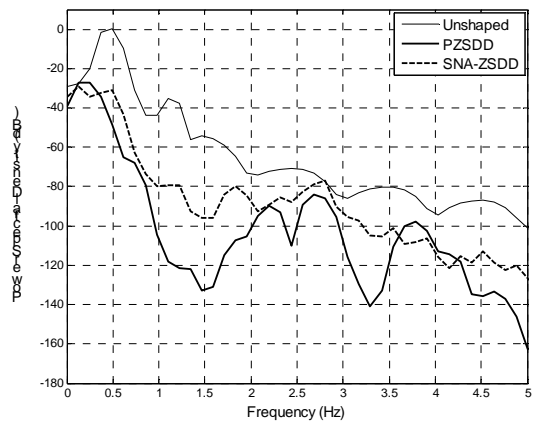

Figure 9: Level of sway reduction for hook swing angle.

Table 1: Level of sway reduction of the hoisting angle of the pendulum and specifications of trolley position response.

Types of shaper (ZSDD)	Swing angle	Attenuation (dB) of sway of the cable			Specification of trolley position response		
		Mode 1	Mode 2	Mode 3	Rise time (s)	Settling time (s)	Overshoot (%)
Positive	Hook swing angle, θ_1	48.85	82.96	75.60	3.252	5.639	0.08
	Load swing angle, θ_2	49.46	86.98	72.12			
Modified SNA	Hook swing angle, θ_1	31.40	43.79	40.57	3.496	5.461	2.36
	Load swing angle, θ_2	31.59	43.21	42.52			
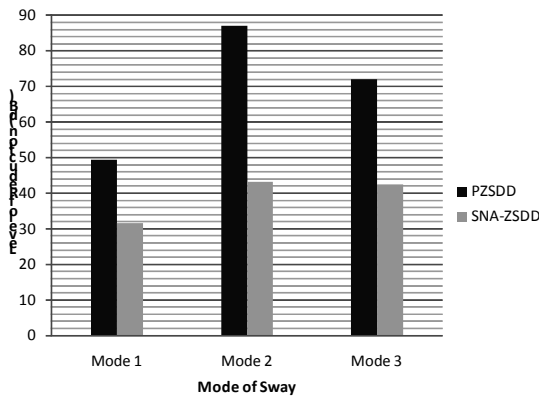
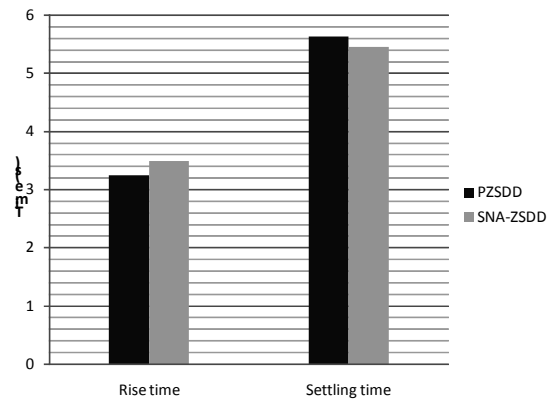Figure 10: Level of sway reduction for load swing angle.

Figure 11: Time response specification.

VI. CONCLUSION

The development of input shaping with different polarities for sway control of a DPTOC system has been presented. The performances of the control schemes have been evaluated in terms of level of sway reduction and time response specifications. Acceptable anti-sway capability has been achieved with both control strategies. A comparison of the results has demonstrated that the positive shapers provide higher level of sway reduction as compared to the cases using modified negative (SNA) shapers. By using the modified negative input shapers (SNA-ZVDD), the speed of the response is slightly improved in term of settling time at the expenses of decrease in the level of sway reduction. It is concluded that the proposed controllers are capable of reducing the system sway while maintaining the steady state position of the trolley.

REFERENCES

[1] Gürleyük, S.S. (2007). Optimal Unity-Magnitude Input Shaper Duration Analysis. Archive of Applied Mechanics, Vol.77, No.1, pp.63-71.

[2] Gürleyük, S.S. and Cinal, Ş. (2007). Robust Three-Impulse Sequence Input Shaper Design. J. of Vibration and Control, Vol. 13, No.12, pp.1807-1818.

[3] Kim, D. and Singhose, W. (2006). Reduction of Double-Pendulum Bridge Crane Oscillations. The 8th International Conference on Motion and Vibration Control, pp. 300-305.

[4] Liu, D.T., Guo, W.P. and Yi, J.Q. (2006) Dynamics and Stable Control for a Class of Underactuated Mechanical Systems. Acta Automatica Sinica, Vol. 32, No. 3, pp. 422-427.

[5] Mohamed, Z., Martins, J.M., Tokhi, M.O., Costa , J.S. and Botto, M.A. (2005). Vibration control of a very flexible manipulator system. Control Engineering Practice, Vol. 13, pp.267-277.

[6] Mohamed, Z., Chee, A.K., Mohd Hashim, A.W I., Tokhi, M.O., Amin, S. H. M. and Mamat, R. (2006). Techniques for vibration control of a flexible manipulator. Robotica, 24, 499-511.

[7] Robertson, M.J. and Singhose, W.E. (2005). Closed-Form Deflection-Limiting Commands. American Control Conference, Portland, USA, pp.2104-2109.

[8] Singer, N.C. and Seering, W.P. (1990) Preshaping Command Inputs to Reduce System Vibration. Journal of Dynamic Systems, Measurement and Control, 112, pp.76-82.

[9] Singhose, W., Crain, E. and Seering, W. (1997) Convolved and Simultaneous Two-Mode Input Shapers. IEEE Proc. Control Theory Appl., Vol. 144, No. 6, pp.515-520.

[10] Singhose, W. and Singer, N. (1996). Effects of Input Shaping on Two-Dimensional Trajectory Following. IEEE Trans. on Robotics and Automation, Vol. 12, No. 6, pp.881-887.

[11] Singhose, W.E., Singer, N.C. and Seering, W.P. (1995). Comparison of command shaping methods for reducing residual vibration. Proceedings of European Control Conference, Rome, pp. 1126-1131.

[12] Smith, O.J.M. (1957). Posicast Control of Damped Oscillatory Systems. Proceedings of the IRE, pp.1249-1255.

[13] Spong, M.W. (1997). Underactuated Mechanical Systems, Control Problems in Robotics and Automation. London: Springer-Verlag.

[14] Tokhi, M.O. and Poerwanto, H. (1996). Control of vibration of flexible manipulators using filtered command inputs. Proceedings of international congress on sound and vibration, St. Petersburg, Russia,, pp. 1019–1026.

[15] Yang, T-S., Chen, K-S., Lee, C-C. and Yin, J-F. (2006). Suppression of Motion-Induced Residual Vibration of a Cantilever

Beam by Input Shaping. J. of Engineering Mathematics, 54, pp.1– 15.